PERILIPIN PROMOTES HSL-MEDIATED ADIPOCYTE LIPOLYSIS VIA PHOSPHORYLATION-DEPENDENT AND INDEPENDENT MECHANISMS

Hideaki Miyoshi[1, 2#], Sandra C. Souza[1#], Hui-Hong Zhang[1], Katherine J. Strissel[1], Marcelo A. Christoffolete[3], Julia Kovsan[4], Assaf Rudich[4], Fredric B. Kraemer[5], Antonio C. Bianco[3], Martin S. Obin[1¶] and Andrew S. Greenberg[1¶]

From the[1] Jean Mayer United States Department of Agriculture Human Nutrition Research Center on Aging, Tufts University, Boston, MA 02111, [2] Hokkaido University Graduate School of Medicine, Sapporo 060-8638, Japan, [3] Brigham and Women's Hospital and Harvard Medical School, Boston MA 02111, [4] Ben-Gurion University, Beer-Sheva, Israel, [5] VA Palo Alto Health Care System and Stanford University, Palo Alto, CA 94305.

Running Title: Perilipin Regulation of HSL Action

¶Correspondence to: Andrew S. Greenberg or Martin S. Obin, Jean Mayer-US Dept. of Agriculture Human Nutrition Research Center on Aging at Tufts University, Boston, MA 02111, Tel: (617) 556-3279, Fax:(617) 556-3224, Email: andrew.greenberg@tufts.edu; martin.obin@tufts.edu

Hormone-sensitive lipase (HSL)[1] is the predominant lipase effector of catecholamine-stimulated lipolysis in adipocytes. HSL-dependent lipolysis in response to catecholamines is mediated by protein kinase A (PKA)-dependent phosphorylation of perilipin A (Peri A), an essential lipid droplet (LD)-associated protein. It is believed that perilipin phosphorylation is essential for the translocation of HSL from the cytosol to the LD, a key event in stimulated lipolysis. Using adipocytes retrovirally engineered from murine embryonic fibroblasts of perilipin null mice (Peri -/- MEF), we demonstrate by cell fractionation and confocal microscopy that up to 50% of cellular HSL is LD-associated in the basal state, and that PKA-stimulated HSL translocation is fully supported by adenoviral expression of a mutant perilipin lacking all six PKA sites (Peri AΔ1-6). PKA-stimulated HSL translocation was confirmed in differentiated brown adipocytes from perilipin null mice expressing an adipose- specific Peri AΔ1-6 transgene. Thus, PKA-induced HSL translocation was independent of perilipin phosphorylation. However, Peri AΔ1-6 failed to enhance PKA-stimulated lipolysis in either MEF adipocytes or differentiated brown adipocytes. Thus, the lipolytic action(s) of HSL at the LD surface requires PKA-dependent perilipin phosphorylation. In Peri -/- MEF adipocytes, PKA activation significantly enhanced the amount of HSL that could be crosslinked to and co-immunoprecipitated with ectopic Peri A. Notably, this enhanced crosslinking was blunted in Peri -/- MEF adipocytes expressing Peri AΔ1-6. This suggests that PKA-dependent perilipin phosphorylation facilitates (either direct or indirect) perilipin interaction with LD-associated HSL. These results redefine and expand our understanding of how perilipin regulates HSL-mediated lipolysis in adipocytes.

The enzymatic hydrolysis of stored neutral lipid in adipocytes is an exquisitely regulated process that maintains whole body energy homeostasis in response to physiological demands. In both white and brown adipose tissue (WAT, BAT) basal (constitutive) rates of adipocyte lipolysis are rapidly and dramatically upregulated by lipolytic hormones such as catecholamines (1,2). In WAT, catecholamine-induced lipolysis provides fatty acids as fuel to peripheral tissues during times of energy need, such as fasting and exercise (3-5). In BAT of human newborns and rodents, catecholamine-stimulated lipolysis provides

fatty acids for heat production (via β− oxidation and mitochondrial uncoupling) in response to hypothermia (i.e., adaptive thermogenesis) (2,6). Fatty acids that are released during adipocyte lipolysis also function as modulators of glucose and insulin action and insulin production (7,8). Moreover, the dysregulated release of fatty acids from adipocytes that occurs in obesity is implicated in the etiology of obesity-related complications, including type 2 diabetes (8-10). Thus, in addition to its role in whole body energy homeostasis, the regulation of adipocyte lipolysis is vital to metabolic health.

Catecholamines stimulate lipolysis by binding to β-adrenergic receptors on adipocytes, resulting in upregulation of adenyl cyclase and activation of PKA (11). PKA activity is thought to increase lipolysis simultaneously by phosphorylating two key substrates: 1) the LD-associated protein, Peri A (12), and 2) HSL, the major lipase in adipocytes with significant hydrolytic action against triacylglyceride (TAG) and diacylglyceride (DAG) (13-15). HSL phosphorylation by PKA increases HSL's catalytic activity, although this increase (2- 3-fold) cannot account for the up to 100-fold increase in adipocyte lipolysis observed following PKA stimulation by catecholamines (15-17). More importantly, PKA-dependent phosphorylation of HSL also promotes HSL translocation from the cytosol to the LD, and the resulting interaction between catalytically active HSL and neutral lipid stores at the LD surface is thought to account for the preponderance of catecholamine-stimulated (vs. basal) lipolysis (16,18). However, the molecular mechanisms by which HSL accumulates at the LD remain unelucidated.

Recent studies have suggested that HSL translocation requires PKA-dependent phosphorylation of Peri A (19). Peri A (the predominant perilipin isoform in adipocytes) is the most prevalent PKA substrate in adipocytes and is a key regulator of both basal and PKA-stimulated lipolysis. *In vitro* and *in vivo* studies demonstrate that reduced levels or absence of perilipin A results in increased basal lipolysis while substantially attenuating catecholamine (PKA)-stimulated lipolysis (20-23). The ability of perilipin to function as both a repressor of basal lipolysis and an enhancer of PKA-stimulated lipolysis has been incorporated into a 'barrier'/translocation model of perilipin function wherein: 1) in the absence of PKA-dependent phosphorylation, perilipin functions as a 'barrier' between stored neutral lipid and lipases such as HSL, thereby maintaining a low rate of basal lipolysis (22-24). The mechanism underlying perilipin's 'barrier' function is undetermined, as perilipin does not form an actual continuous physical barrier around LDs (25); 2) PKA-dependent perilipin phosphorylation at six serine residues (consensus PKA sites) is required for stimulated lipolysis (14,22,26), presumably reflecting perilipin conformational changes that expose stored neutral lipid and facilitate HSL translocation to the LD (19,22,27). This combination of abrogated 'barrier' function and facilitation of HSL translocation is proposed as the mechanism by which PKA-dependent perilipin phosphorylation mediates catecholamine- stimulated lipolysis in adipocytes (19,22,23,27). This model is called into question, however, by the observation that significant levels (up to ~50%) of HSL are associated with adipocyte LDs under basal conditions (25,28,29) and by the fact that bulk translocation of HSL is not a consistent feature of hormone-stimulated lipolysis (30,31).

The present study provides the first empirical dissection of the coincident effects of blocking perilipin phosphorylation on both HSL translocation and lipolysis. Employing adenoviral and transgenic expression of a perilipin construct deficient in all six PKA sites (Peri AΔ1-6), we demonstrate that PKA-dependent phosphorylation of perilipin is not required for HSL translocation to the LD, but is essential for the lipolytic action(s) of LD-associated HSL in adipocytes. Crosslinking and immunoprecipitation studies suggest that PKA-dependent phosphorylation of perilipin promotes close-range interaction with LD-associated HSL. These observations redefine the mechanism by which perilipin regulates HSL-mediated lipolysis in response to β-adrenergic stimuli.

EXPERIMENTAL PROCEDURES

Antibodies— A polyclonal anti-perilipin antibody (22,23) and a polyclonal anti-HSL antibody (32) were generated as previously described. A polyclonal antibody (cat. # 9621) recognizing phosphorylated serine/threonine residues of concensus PKA sites was purchased from Cell Signaling Technology, Inc. (Beverly, MA). Rabbit anti-NAD(P)H steroid dehydrogenase-like protein (Nsdhl) (33) was generously provided by Dr. Masato Ohashi, National Institute for Physiological Sciences, Okazaki, Japan). A mouse monoclonal antibody specific for adiponectin was from Affinity BioReagents™ (Golden, CO). A rabbit polyclonal antibody against clathrin was from BD Biosciences (San Jose, CA). Horseradish-linked anti-rabbit IgG was purchased from Amersham Biosciences (Piscataway, NJ). Alexa Fluor 647-conjugated goat anti-rabbit IgG was purchased from Molecular Probes (Eugene, OR).

Perilipin knockout (Peri KO) mice and Peri KO mice expressing the Peri AΔ1-6 transgene in BAT (Peri AKOΔ1-6 mice)— We generated mice with a targeted disruption of the perilipin gene by replacing exon 3 (nucleotides 3515 and 3887) with a neomycin cassette, thereby disrupting coding of all known perilipin mRNAs. The Peri KO mice were viable and exhibited predicted reductions in adipocyte size and adipose mass as previously described (20,21). Peri KO mice were backcrossed for 10 generations to C57BL/6 mice (Harlan, Indianapolis, IN). We subsequently generated mice expressing a Peri AΔ1-6 transgene in adipose tissue. We first generated a mouse Peri AΔ1-6 cDNA, FLAG-tagged at the carboxy terminal using PCR (23). This cDNA was then ligated into a SmaI site of pBluescript SK vector containing the aP2 enhancer/promoter region, the SV40 small tumor antigen splice site and polyadenylation signal sequence (a gift of Dr. B.M. Spiegelman) (34). A fragment containing the entire aP2-Peri A-FLAG transgene was microinjected into fertilized eggs of C57BL/6 mice. The general procedure for microinjection of the transgene is described elsewhere (35). Transgenic mice expressing the Peri AΔ1-6 transgene almost exclusively in BAT were obtained. These mice were fully viable and exhibited no overt adipose phenotype (data not shown). These transgenic mice were mated with backcrossed Peri KO mice to generate Peri AKOΔ1-6 mice used in these studies.

Generation and differentiation of stable lines of MEF adipocytes— Stable lines of MEF adipocytes were generated from 12.5-14.5 d embryos of Peri +/+ and Peri -/- mice as described (36). Retrovirus expressing mouse PPARγ in a pMSCV vector (Clontech, Mountain View, CA) were generously provided by Dr. Evan Rosen and transfected into phoenix cells using the manufacturer's instructions. Viral supernatants were added to MEF cells for 4 h, selected with puromycin, expanded, and frozen for later use. Selected MEF cells were cultured in Dulbecco's modified Eagle's medium (DMEM) with 10% fetal bovine serum (FBS). At confluence cells were exposed to a pro-differentiation regimen of dexamethasone (1 μM), insulin (5 μg/ml), isobuthylmethylxanthine (IBMX, 0.5 mM), and rosiglitazone (5 μM). After 2 d, cells were maintained in medium containing insulin for 4 d, then in medium without insulin for an additional 3-4 d before use.

Recombinant Adenoviruses— Serine to alanine mutations were made in all six Peri A PKA sites (Ser81, Ser222, Ser276, Ser433, Ser492, and Ser517) using Muta-Gene Phagemid *in vitro* mutagenesis version 2 (Bio-Rad, Hercules, CA). Adenoviruses expressing this construct (Ad Peri AΔ1-6), wild type perilipin (Ad Peri A) or Aequoria Victoria green fluorescent protein (Ad GFP, a control for nonspecific adenoviral effects), were generated using the AdEasy™ adenoviral vector system (Stratagene, La Jolla, CA) (23). Wild type perilipin and Peri AΔ1-6 were FLAG-tagged at the C- terminus. Adenoviruses were amplified in HEK 293 cells and purified and concentrated to 0.6×10^{12} plaque-forming units/ml by CsCl ultracentrifugation.

Isolation and in vitro differentiation of brown

preadipocytes— Brown fat precursor cells were isolated from the interscapular brown adipose tissue of 5-6 week old C57BL/6 and Peri AKOΔ1-6 mice as previously described (37). Cells were cultured in maintenance medium (DMEM medium containing 10% FBS, supplemented with 10 mM HEPES, 100 nM sodium selenite, 3 nM insulin, 15 mM ascorbic acid, 50 mg/L tetracycline, 50 mg/L streptomycin, 50 mg/L ampicillin and 1 mg/L Fungizone (Invitrogen, Carlsbad, CA)). Precursors were seeded at 15-20,000 cells/cm^2 in 12-well plates or in 35-mm coverslip-bottom dishes for lipolysis and immunostaining studies, respectively. After they attained confluence (d 0), cells were cultured for 2 d in differentiation medium (DMEM containing 0.5 mM IBMX, 0.5 mM dexamethasone and 125 μM indomethacin (38)), after which they were maintained in maintenance medium for an additional 3 d before assays.

Recombinant adenovirus expressing small hairpin RNA (shRNA) for murine HSL— HSL shRNA design was based on accession number NM010719 (sequence: GCAAGAGTATGTC ACGCTA) (Welgen, Inc., Worcester, MA). A 'scrambled' version of this HSL shRNA (CGCGCTTTGTAGGATTCA) was also generated as a control for nonspecific effects of shRNA on lipolysis. Both HSL shRNA and the 'scrambled' shRNA were cloned into the pQuiet vector to generate recombinant adenoviruses.

Adenovirus-mediated expression of perilipins or shRNAs in MEF -/- adipocytes— Recombinant adenovirus was transduced in peri -/- MEFs with LipofectAMINE Plus™ reagent (Invitrogen) on d 2 (shRNA) or 3 (perilipins) after induction of differentiation. To assure comparable levels of adenovirally-induced protein expression, each adenovirus was pre- and post-titered using Western blots and densitometry of cell lysates (22).

Lipolysis assays— Prior to lipolysis assays, differentiated brown adipocytes were incubated overnight in insulin/serum-free medium with 2% fatty acid-free BSA (DMEM/BSA). MEF adipocytes were incubated for ≥ 4 h in the same medium. For lipolysis assays, adipocytes were incubated for either 40 min (brown adipocytes) or 2 h (MEF adipocytes) in DMEM/BSA containing 200 nM phenyl isopropyl adenosine (PIA) (basal condition) or in PIA and 10 μM norepinephrine (NE) (brown adipocytes) or PIA and 20 μM forskolin (MEF adipocytes). The medium was then collected and established procedures were used to quantify glycerol and fatty acids as indices of HSL-mediated and total lipolysis, respectively (22,39).

Insulin-dependent glucose uptake— Insulin dependent glucose uptake was measured in MEF adipocytes using insulin and the 2-[^{3}H]deoxyglucose uptake assay as previously described (40).

Immunofluorescence microscopy— After serum depletion, cells were treated for 15 min with either 200 nM PIA to repress adenyl cyclase activity (basal condition) or with 20 μM forskolin plus 0.5 mM IBMX (stimulated condition), followed by fixation and incubation with antibodies recognizing either perilipin or HSL. Differentiated brown adipocytes were treated for 15 min with either 200 nM PIA or 10 μM NE. Images were acquired with a Leica TCS SP2 confocal microscope equipped with an acoustico-optical beam splitter.

Subcellular fractionation— Differentiated MEF-/- adipocytes were incubated in differentiation medium containing palmitic and oleic acid (240 μM each) for 48 h. After overnight serum depletion, adipocytes were treated for 13 min with 200 nM PIA (basal state) or 20 μM forskolin plus 0.5 mM IBMX (stimulated state), washed with PBS and then maintained for 10 min in hypotonic buffer (20 mM Tris-HCl (pH 7.5)) containing 2 mM EDTA, 50 mM sodium fluoride, 100 μM sodium ortho-vanadate, protease inhibitor cocktail (Sigma, St. Louis, MO), and either PIA or forskolin plus IBMX. Cells were homogenized on ice, and homogenates were centrifuged (12,000 rpm) at 4°C for 20 min to

separate fat cake (FC, upper layer containing lipid droplets) or supernatant (SP, lower layer) and a membrane pellet. The FC layer was isolated with a tube cutter and placed in a fresh tube. The SP was subjected to multiple rounds of centrifugation and removal of the residual FC, until almost no FC fraction was visible. Then the lower portion of the SP fraction was harvested by needle aspiration and removed to a fresh tube. The pooled FC fractions were washed with 1 ml of fresh lysis buffer, collected (as above) after centrifugation and resuspended in fresh lysis buffer. Half of this FC suspension was used for TAG measurement. The remaining half was incubated with SDS lysis buffer (10% final) at 37°C for 30 min with vortexing and then centrifuged for 10 min, after which the final FC fraction was harvested. One-thirtieth (by volume) of each fraction was loaded on SDS-PAGE gels and then Western blotted for perilipin and HSL. The FC isolation procedure resulted in minor differences in the total FC fraction recovered. Therefore, FC sample volumes were adjusted based on TG content to insure that equivalent amounts of FC were loaded from basal and PKA-stimulated samples.

Perilipin–HSL crosslinking and co-immunoprecipitation— Differentiated MEF -/- adipocytes expressing GFP, FLAG-tagged Peri A, or FLAG-tagged Peri AΔ1-6 were incubated as described (above) for cell fractionation studies with the exception that Hepes (pH 7.4) replaced Tris in the hypotonic buffer. Cells were then harvested and hand-homogenized on ice. 3,3'-Dithiobis sulfosuccinimidyl propionate (DTSSP), a cross-linker with 12Å spacer arm length (Pierce, Rockford, IL) was added to the homogenates and incubated with rotation at room temperature for 30 min as per manufacturer's instructions. The cross-linking reaction was terminated by addition of Tris-HCl (50 mM final). After addition of Triton X-100 (2% final) and NaCl (75 mM final), samples were drawn through a 23 gauge needle and then centrifuged (12,000 rpm) at 4°C for 20 min. The supernatant and FC were purified as for the subcellular fractionation studies (see above). Western blotting confirmed that > 95% of perilipin was removed from the LD and present in the SP fraction. The SP fraction was immunoprecipitated using the FLAG® Tagged Protein Immunoprecipitation Kit (Sigma) at 4°C for 24 h with rotation. Immunoprecipitates were eluted from pelleted anti-FLAG agarose beads by boiling in SDS-PAGE sample buffer containing the reducing agent 2-mercaptoethanol. The reducing conditions are sufficient to break the DTSSP-induced protein crosslinks. Eluted samples were electrophoresed and immunoblotted for the LD-associated proteins perilipin, HSL and Nsdhl. To assess potential nonspecific cross-linking of perilipin with membrane or cytosolic proteins, immunoblots were also probed with antibodies to clathrin and adiponectin.

Statistical analysis— Results are expressed as mean ± S.E. Differences between treatments were analyzed by ANOVA using Bonferroni protections for multiple comparisons (STAT view v5.0 for Macintosh, SAS Institute). Percentage data for HSL cellular distribution (Table 1) were transformed as arcsin √X before ANOVA (41).

RESULTS

Characterization of Peri -/- MEF Adipocytes

Our experimental strategy was to develop a stable line of perilipin null adipocytes in which to examine the effects of ectopically-expressed wild type or PKA site-deficient perilipin on HSL translocation and HSL-mediated lipolysis. We generated a stable line of adipocytes from MEFs of wild type and Peri -/- mice using retroviral expression of mouse PPARγ in both lines to drive adipogenesis (see Experimental Procedures). To confirm that the absence of Peri A in Peri -/- MEFs did not significantly alter adipogenesis, we compared the differentiation time-course and hallmark adipocyte phenotypes in Peri +/+ and Peri -/- adipocytes. We confirmed that the time-course of adipogenesis was identical in Peri +/+ and Peri -/- MEF adipocytes, with both lines

differentiating into mature adipocytes by 9 d of culture (Fig. 1A). At this time, both Peri +/+ and Peri -/- MEF adipocytes exhibited robust expression of characteristic adipocyte proteins, including adiponectin and HSL (Fig. 1A, left panel) as well as Glut 4, adipocyte triglyceride lipase and adiponutrin (data not shown). Expression levels of hallmark adipocyte proteins in Peri -/- MEF adipopcytes were comparable to levels observed for Peri +/+ MEF adipocytes (Fig. 1A, right panel). Peri -/- MEFs also exhibited physiological characteristics of mature adipocytes, including TAG accumulation in LDs (Fig. 1B) and ≥ 4-fold increase in glucose uptake in response to insulin (Fig. 1C). In addition, forskolin-stimulated activation of PKA upregulated lipolysis ~12-fold in Peri -/- MEF adipocytes ectopically expressing Peri A (see below). The magnitude of forskolin-stimulated lipolysis was comparable to that obtained with Peri +/+ MEF adipocytes (11.5- fold) and with 3T3-L1 adipocytes (8-15- fold) (data not shown). In summary, we were able to successfully generate a stable line of Peri -/- MEF adipocytes which exhibit typical molecular and physiological characteristics of adipocytes.

Lipolytic Actions of Peri A and Peri AΔ1-6 in Peri -/- MEF Adipocytes

We next utilized adenoviral gene delivery to assess the effects of Peri A and Peri AΔ1-6 on lipolysis in differentiated Peri -/- MEF adipocytes. As a control for the potential confounding effects of adenoviral infection, a third group of MEF -/- adipocytes were infected with an adenovirus expressing GFP. In the Peri AΔ1-6 protein, serine residues comprising the six consensus PKA sites are mutated to alanine (Fig. 2A). Based on prior studies in lipid-loaded fibroblasts ectopically expressing HSL, we predicted that both Peri A and Peri AΔ1-6 would block basal lipolysis, but only Peri A would support PKA- stimulated lipolysis (23). Western blot analysis demonstrated that Peri A and Peri AΔ1-6 were expressed at comparable levels (Fig. 2B, compare lanes 3 and 5). However, only Peri A was hyperphosphorylated in response to the PKA activator forskolin (Fig. 2B, compare lanes 4 and 6). Perilipin hyperphosphorylation is manifest on Western blots as the formation of a slower migrating upper band. The presence of two perilipin bands gives the appearance of increased protein levels as compared with nonphosphorylated perilipin (Fig. 2B, lanes 3, 5 and 6).

In lipolysis assays, both Peri A and Peri AΔ1-6 reduced basal lipolysis (measured as glycerol release) as compared with MEFs expressing GFP ($P < 0.001$; Fig. 2C). The inhibitory effects of Peri A and Peri AΔ1-6 on basal lipolysis were essentially identical ($P = 0.42$). This result is consistent with prior demonstration in non-adipocyte cell lines that the perilipin's ability to block basal lipolysis does not require phosphorylation of PKA sites (23). Forskolin treatment increased lipolysis approximately 1.6-fold (vs. basal) in Peri -/- adipocytes transduced with GFP adenovirus, suggesting that a perilipin-independent mechanism mediates a modest level of PKA-dependent lipolysis in MEF adipocytes (20,21) (Fig. 2C). In contrast, ectopic expression of Peri A in Peri -/- adipocytes increased forskolin-stimulated lipolysis ~12-fold as compared with basal lipolysis, confirming the predominant role of perilipin in PKA-stimulated lipolysis. In contrast, forskolin-stimulated lipolysis in Peri -/- adipocytes expressing Peri AΔ1-6 attained only the level observed for Peri -/- MEF adipocytes expressing GFP ($P = 0.52$; Fig. 2C). Thus, the perilipin-dependent enhancement of PKA-stimulated lipolysis that was observed with wild type Peri A was absent. This result confirms that one or more perilipin PKA sites are required for perilipin-dependent enhancement of lipolysis in response to PKA.

HSL shRNA Abrogates The Preponderance of Perilipin-Dependent, PKA-Stimulated Lipolysis in MEF Adipocytes

In previous studies using lipid-loaded fibroblast cell lines (23), we observed that up to one-third of total perilipin-mediated PKA-stimulated lipolysis (glycerol release) could be accounted for by unidentified lipase(s) other than HSL. Here, we employed a shRNA strategy to determine the relative contribution of HSL and non-HSL lipases to

PKA-stimulated glycerol release in MEF adipocytes. Expression of HSL-directed shRNA in MEF -/- adipocytes transduced with Peri A adenovirus reduced HSL protein levels by > 90% compared with the expression of 'scrambled' shRNA (Fig. 3A, compare lanes 3 and 4 with lanes 5 and 6). This reduction in HSL protein expression was associated with comparable (92%) attenuation of forskolin-stimulated glycerol release to levels almost identical to those measured in MEF -/- adipocytes expressing GFP ($P = 0.67$; Fig. 3B). Thus, glycerol release from MEF -/- adipocytes provides a robust assay for investigating the role of perilipin phosphorylation in PKA-stimulated HSL translocation and HSL-mediated lipolysis.

HSL shRNA blocked 77% of PKA-stimulated fatty acid release (from 2.82 ± 0.55 μEq/mg protein to 1.20 ± 0.12 μEq/mg protein). The residual (23%) fatty acid release relative to Peri -/- adipocytes expressing GFP (0.73 ± 0.13 μEq/mg protein; $P = 0.01$) implicates an additional lipase(s) in PKA-stimulated fatty acid release in our MEF adipocytes.

Elucidating the Role of Perilipin and Perilipin Phosphorylation in PKA-stimulated HSL Translocation and Lipolytic Action

It has been proposed that PKA-dependent phosphorylation of perilipin promotes lipolysis in large part by facilitating HSL translocation from the cytosol to the LD (16,18). This currently accepted model predicts that in the absence of perilipin hyperphosphorylation (basal state, or in the presence of Peri AΔ1-6), HSL would be prevented from translocating from the cytosol to the LD, resulting in low rates of lipolysis. To directly test this model, we investigated the subcellular localization of HSL in response to PKA activation in MEF -/- adipocytes expressing our adenoviral constructs. These investigations used cell fractionation and Western blotting in conjunction with confocal microscopy of immunofluorescent stained cells. Cell fractionation studies of Peri -/- adipocytes expressing GFP revealed that in the basal state (absence of forskolin), most (~95%) of HSL is located in the supernatant, although some HSL appears to be associated with the 'fat cake' (Fig. 4, top row, A: compare lanes 1 and 2; Table 1). Addition of forskolin did not increase HSL association with the FC fraction (Fig. 4, top row, A: compare lanes 3 and 4 with lanes 1 and 2; Table 1). Confocal studies confirm that in the absence of either wild type or mutant perilipin, most HSL immunofluorescence is localized to the non-LD compartment in both basal and stimulated states (Fig. 4, top row, B: compare panels 1 and 2 with panels 3 and 4).

In Peri -/- MEF adipocytes expressing Peri A, approximately half of cellular HSL was associated with the FC fraction in the absence of forskolin ($P < 0.001$ vs GFP; Fig. 4, middle row, A: compare lanes 1 and 2; Table 1). However, consistent with the ability of Peri A to block basal lipolysis, this perilipin-dependent increase in FC-associated HSL was coincident with *reduced* lipolysis as compared with MEF-/- adipocytes expressing GFP (Fig. 2C). The addition of forskolin to MEF -/- adipocytes expressing Peri A resulted in a 25-30% relative increase in the proportion of HSL in the FC fraction ($P < 0.05$; Fig. 4, middle row, B: compare lanes 3 and 4 with lanes 1 and 2; Table 1). This PKA-dependent increase in the relative proportion of FC-associated HSL is confirmed in confocal images by the appearance of less diffuse, bright rings of green fluorescence around LDs (Fig. 4, middle row, B: compare panels 3 and 4 with panels 1 and 2). The PKA-dependent increase in LD-associated HSL in Peri -/- MEF adipocytes expressing Peri A is coincident with enhanced lipolysis (Fig. 2C).

We next examined HSL cellular localization in MEF -/- adipocytes expressing Peri AΔ1-6. Comparable to wild type Peri A, Peri AΔ1-6 supported the basal state association of ~50% of cellular HSL with the FC fraction, a significant increase over levels observed with GFP ($P < 0.001$) (Fig. 4A: compare bottom row lanes 1 and 2 with top row lanes 1 and 2; Table 1). This perilipin-dependent increase in HSL in the FC fraction was associated with reduced basal lipolysis (Fig. 2C). Most surprisingly, Peri AΔ1-6 supported a 43% relative increase in HSL association with the FC fraction in response to forskolin ($P < 0.01$) (Fig. 4A:

bottom row, compare lanes 3 and 4; Table 1). Importantly, this PKA-induced increase in FC-associated HSL was as great as the increase observed in MEF -/- cells expressing Peri A (Table 1; P = 0.67). This unexpected PKA-dependent increase in FC-associated HSL in Peri AΔ1-6 adipocytes was confirmed by the appearance in confocal images of bright rings of HSL immunofluorescence around LDs (Fig. 4B: bottom row, compare panels 3 and 4 with panels 1 and 2). Thus, mutation of perilipin PKA sites had no observable effect on the ability of HSL to translocate to the LD in response to PKA activation. Yet, mutation of perilipin PKA sites fully blocked the enhancement of PKA-stimulated lipolysis (Fig. 2C).

Together, results from lipolysis and translocation studies indicate that perilipin, *but not PKA-dependent perilipin phosphorylation,* is required for HSL translocation to and association with the LD. However, PKA-dependent perilipin phosphorylation *is* required for the lipolytic action of LD-asociated HSL (and perhaps other lipases).

Distinct Roles of Perilipin and Perilipin Phosphorylation in HSL Translocation and HSL-Mediated Lipolysis Are Confirmed in Differentiated Brown Adipocytes from Peri AKOΔ1-6 Transgenic Mice

As part of studies to elucidate the *in vivo* role of perilipin phosphorylation in PKA-stimulated lipolysis, we generated perilipin knockout mice that express a FLAG-tagged Peri AΔ1-6 transgene in brown adipocytes (Peri AKOΔ1-6 mice). We used *in vitro* differentiated brown adipocytes from these transgenic (and wild type) mice to verify and extend our observation that PKA-dependent perilipin phosphorylation is not required for PKA-induced HSL translocation, but is required for HSL's lipolytic action at the LD surface. Differentiated brown adipocytes from wild type and Peri AKOΔA1-6 mice expressed protein markers of mature brown adipocytes, including perilipin, HSL and uncoupling protein-1 (UCP1) (Fig. 5A). Perilipin levels were ~2-fold greater in differentiated brown adipocytes from Peri AKOΔ1-6 mice than from wild type mice. We previously reported that overexpression of perilipin up to 4-fold vs. wild type levels of expression has no detectable effect on differentiation, viability or lipolysis in 3T3-L1 adipocytes (42). Differentiated brown adipocytes acquired the characteristic rounded adipocyte morphology with intracellular TAG stored in LDs (Fig. 5B). Moreover, in response to physiologically relevant PKA stimulation by NE, PKA site-specific phosphoserine content of wild type Peri A increased, whereas no PKA site-specific phosphoserine content was detected in Peri AΔ1-6 (Fig. 5A). This result confirms that Peri AΔ1-6 is not phosphorylated by PKA in response to catecholamines in differentiated brown adipocytes derived from Peri AKOΔ1-6 mice. Consistent with the abrogation of PKA-dependent phosphorylation, lipolysis assays revealed a ~90% block of NE-stimulated glycerol release in Peri AKOΔ1-6 adipocytes as compared with wild type adipocytes (P < 0.001; Fig. 5B). Specifically, whereas NE treatment stimulated lipolysis 3.2-fold in wild type adipocytes, NE stimulated lipolysis only 1.3-fold in Peri AKOΔ1-6 adipocytes (Fig. 5B). However, this 30% increase in glycerol release was statistically significant relative to basal state release (P = 0.02; Fig. 5B).

We next assessed perilipin and HSL localization in wild type and Peri AKOΔ1-6 brown adipocytes employing confocal, differential interference contrast (DIC) and immunofluorescence (IF) microscopy (Fig.6). Perilipin IF (red; column 2) demonstrates that Peri AΔ1-6 localizes exclusively to LDs similar to wild type Peri A in brown adipocytes. HSL IF (Fig. 6, column 3) reveals that in the basal state, HSL localizes to both the cytoplasm and LDs in wild type and Peri AKOΔ1-6 adipocytes, as indicated by diffuse green fluorescence surrounding LDs. Colocalization of perilipin and HSL is manifest as orange color in the Peri A/HSL overlay images (Fig. 6, column 4). This HSL association with the LD in the basal state is consistent with our observations in the MEF studies of Figure 4.

In response to NE treatment, HSL immunofluorescence (green) becomes less diffuse, and bright distinct rings of green immunofluorescence are observed in both wild type and Peri AKOΔ1-6 adipocytes, an

indication of increased LD-associated HSL (Fig. 6, column 3). The proportional increase in LD-associated HSL produces a yellow color in the HSL/Peri A overlay images (Fig. 6, column 4). Thus, in differentiated brown adipocytes as in MEF adipocytes, the PKA-stimulated increase in LD-associated HSL does not require PKA-dependent perilipin phosphorylation. However, in both differentiated brown adipocytes (Fig. 5B) and MEF adipocytes (Figs. 2 and 3), PKA-stimulated lipolysis requires phosphorylation of one or more perilipin PKA sites.

Perilipin Phosphorylation Promotes Close Interaction of LD-associated HSL with Perilipin

The requirement of perilipin for quantitative HSL association with the LD (Fig. 4), suggested that HSL might bind to perilipin (either directly or indirectly) and that perilipin phosphorylation might promote HSL's lipolytic action at the LD by altering this interaction. To examine this possibility, we performed crosslinking and perilipin immunoprecipitation studies in Peri -/- MEF adipocytes expressing the (FLAG-tagged) Peri A or Peri AΔ1-6 constructs used for the lipolysis and translocation studies above. Crosslinking was used because solubilization of LD proteins for immunoprecipitation requires detergents or chaotropic agents, which disrupt protein-protein interactions (see Experimental Procedures). Chemical crosslinking stabilizes these interactions. Following immunoprecipitation with anti-FLAG antibody, immunoprecipitates were Western blotted for perilipin and for co-immunoprecipitated HSL.

Both Peri A and Peri AΔ1-6 were successfully immunoprecipitated from MEF adipocytes (Fig. 7A, upper panel). Immunoprecipitation was quantitative, removing 60-80% of perilipin from adipocyte lysates, based on densitometric comparison of pre-and post-IP lysates (data not shown). In the basal state, low levels of HSL were co-immunoprecipitated with either Peri A or Peri AΔ1-6 (Fig. 7A, lanes 3 and 5). When normalized to perilipin levels (assessed by densitometry), basal state levels of co-immunoprecipitated HSL were comparable between wild type perilipin and Peri AΔ1-6 (data not shown). These observations suggest that a small amount of LD-associated HSL is closely-associated with perilipin in the basal state. Forskolin treatment of Peri -/- MEF adipocytes expressing wild type perilipin resulted in a dramatic (6-8-fold) increase in co-immunoprecipitated HSL as compared with the basal state (Fig. 7A, compare lanes 3 and 4). These results suggest that PKA-dependent perilipin phosphorylation alters the spatial relationship between Peri A and LD-associated HSL in such a manner as to facilitate HSL-Peri A crosslinking over that observed in the absence of perilipin phosphorylation. This cross-linking is quantitative, as ~30-35% of total HSL was co-immunoprecipitated with Peri A from lysates of forskolin-treated cells expressing Peri A, based on densitometry and adjusted for nonspecific HSL loss in the presence of GFP (~7%) (data not shown). The figure of 30-35% is comparable to half of the LD-associated HSL in forskolin-stimulated MEF adipocytes (Table 1).

The importance of Peri A phosphorylation to enhanced HSL-Peri A crosslinking is underscored by our observation that forskolin treatment of Peri -/- MEF adipocytes that express Peri AΔ1-6 resulted in only a modest (2-fold) increase in co-immunoprecipitated HSL, presumably reflecting direct effects of PKA on HSL (27) (Fig. 7A, compare lanes 5 and 6). Thus, abrogation of PKA-dependent Peri A phosphorylation substantially (≥ 3-fold) reduced the amount of HSL that was crosslinked to Peri A under the experimental conditions reported here. Consistent with this result, only ~8% of HSL was specifically co-immunoprecipitated with Peri AΔ1-6 from lysates of forskolin-treated cells (data not shown).

Importantly, Western blots of perilipin immunoprecipitates were negative for the LD-associated protein, NAD(P)H steroid dehydrogenase-like protein (Nsdhl) (33), demonstrating that co-immunoprecipitation of HSL and perilipin in these experiments does not reflect promiscuous crosslinking of

perilipin with all LD-associated proteins (Fig. 7B). In addition, Western blots of immunoprecipitates were negative for clathrin and adiponectin (i.e., proteins that are not LD-associated), although these proteins were readily detected in MEF supernatants from which perilipin was immunoprecipitated (data not shown). It is therefore unlikely that HSL co-immunoprecipitation with perilipin in these experiments reflects crosslinking of cytosolic HSL to perilipin. Finally, neither HSL nor perilipin were immunoprecipitated from Peri -/- MEF adipocytes expressing GFP (Fig. 7A, lanes 1 and 2), arguing against nonspecific binding of HSL to the agarose beads used for immunoprecipitation.

These results in conjunction with data from lipolysis assays (Figs. 2 and 3) suggest that 1) PKA-dependent perilipin phosphorylation promotes close range interaction of LD-associated HSL with perilipin, and 2) this interaction contributes to PKA-stimulated lipolysis.

DISCUSSION

It was previously held that PKA-dependent perilipin phosphorylation was required to induce HSL translocation from the cytosol to the LD, an event critical to hormone-stimulated lipolysis in adipocytes (19,27). We evaluated the requirement for perilipin phosphorylation in HSL translocation using two types of differentiated adipocytes: 1) adipocytes developed from MEFs of perilipin knockout mice; these adipocytes were transduced with adenovirus to express either wild type perilipin (Peri A) or PKA site-deficient perilipin (Peri AΔ1-6); and 2) adipocytes differentiated from BAT preadipocytes of perilipin knockout mice expressing the Peri AΔ1-6 transgene in BAT. These two adipocyte model systems allowed us to dissect and distinguish effects of perilipin and perilipin phosphorylation on HSL association with the LD and with HSL-mediated lipolysis, respectively.

Our studies demonstrate that perilipin promotes HSL-mediated adipocyte lipolysis via discrete phosphorylation-independent and phosphorylation-dependent mechanisms. A phosphorylation-independent mechanism(s) mediates HSL association with the LD in the basal state, as well as HSL translocation from the cytosol to the LD in response to PKA activation (Figs. 4 and 6). These observations confirm prior reports that Peri A is required for HSL association with the LD (19). In response to PKA, the amount of LD-associated HSL increases relative to the basal state, reflecting the translocation of phosphorylated HSL from the cytosol to the LD and its perilipin-dependent arrest at the LD. Importantly, we demonstrate for the first time that this PKA- and perilipin-dependent increase in LD-associated HSL does not require PKA-dependent Peri A phosphorylation. It remains unclear how perilipin promotes HSL arrest at the LD, either in the basal state or following HSL translocation from the cytosol. The mechanism may be indirect. For example, Peri A may facilitate the formation of LDs of a certain size, curvature or protein composition, and HSL may preferentially associate with such LDs, as recently suggested (25). Irrespective of the mechanism involved, our data do not support the proposed role of Peri A phosphorylation in PKA-induced HSL translocation (17,19). This discrepancy is likely to reflect the fact that studies suggesting a requirement of perilipin phosphorylation for HSL translocation were conducted in a non-adipocyte cell line (Chinese hamster ovary cells) which does not express endogenous perilipin or HSL and is not specialized for TAG storage or hydrolysis (19).

With respect to the phosphorylation-dependent mechanism by which perilipin promotes lipolysis, the present study reveals that the lipolytic action(s) of LD-associated HSL require a novel event(s) mediated by PKA-dependent perilipin phosphorylation (Figs. 2C and 5B). The precise nature of this event(s) remains to be elucidated. However, it is likely to involve conformational changes in perilipin that bring LD-associated HSL into proximity with stored neutral lipid. The effected LD-associated HSL presumably includes the pool of HSL that is pre-positioned at the LD in the basal state (Fig. 4A and Table 1) (25,28,29). Our crosslinking studies (Fig. 7)

suggest that PKA-dependent phosphorylation of perilipin alters the spatial relationship between perilipin and LD-associated HSL in such a way as to facilitate close-range interaction between the two (or between HSL and a perilipin-associated moiety). This interaction may facilitate access of LD-associated HSL to stored neutral lipid, thereby initiating lipolysis. While the present study was in review, Brasaemle and colleagues reported that chronic PKA-dependent phosphorylation of Peri A induced LD remodeling (i.e., fragmentation and dispersion) independently of lipase action and suggested that this remodeling promoted lipolysis (43). These observations support the concept that PKA-dependent phosphorylation induces dramatic conformational changes in perilipin. However it is currently undetermined if PKA-induced LD remodeling is mechanistically related to the altered HSL-Peri A interaction suggested by the present study.

In summary, the present study supports an emerging view of perilipin as the critical component of a scaffold that stabilizes LD structure and composition for optimal lipid storage and regulated lipolysis (25,29). The scaffold is dynamic. In the basal state it arrests HSL (and perhaps other lipases) at the LD, but precludes lipolysis, ostensibly by sequestering HSL from neutral lipid stores. In response to hormonal activation of PKA the scaffold brings LD-associated HSL into sufficiently close proximity to lipid substrate to affect PKA-stimulated lipolysis. This function of the scaffold requires PKA-dependent perilipin phosphorylation. These and other functions of the lipolytic scaffold are likely to require the interplay of perilipin with lipid substrate(s) and /or other LD-associated proteins that remain to be identified.

Acknowledgements: This work was supported by grant NIH DK-50647 and U. S. Department of Agriculture–Agricultural Research Service Co-Operative Agreement 58 1950-4-401 (ASG), NIH AG024635, GRASP Center P30 DK-34928 and the American Diabetes Association (MSO), Tufts Center for Neuroscience Research, P30 NS047243 (Jackson), the Research Service of the Department of the Veterans Affairs (FBK), and Grant #2003088 from the US-Israel Binational Science Foundation (ASG and AR). HM thanks Professor Takao Koike for his continued support and mentorship. We thank three anonymous reviewers for thoughtful comments.

REFERENCES

1. Tansey, J. T., Sztalryd, C., Hlavin, E. M., Kimmel, A. R., and Londos, C. (2004) *IUBMB Life* **56**, 379-385
2. Robidoux, J., Martin, T. L., and Collins, S. (2004) *Annu Rev Pharmacol Toxicol* **44**, 297-323
3. Coppack, S. W., Jensen, M. D., and Miles, J. M. (1994) *J Lipid Res* **35**, 177-193
4. Arner, P. (1995) *Int J Obes Relat Metab Disord* **19**, S18-21
5. Dodt, C., Lonnroth, P., Wellhoner, J. P., Fehm, H. L., and Elam, M. (2003) *Acta Physiol Scand* **177**, 351-357
6. Sell, H., Deshaies, Y., and Richard, D. (2004) *Int J Biochem Cell Biol* **36**(11), 2098-2104
7. Frayn, K. N. (2003) *Biochem Soc Trans* **31**, 1115-1119
8. Arner, P. (2005) *Best Pract Res Clin Endocrinol Metab* **19**, 471-482
9. Shulman, G. (2000) *J Clin Invest* **196**, 171-176
10. Wyne, K. L. (2003) *Am J Med* **115**, 29S-36S
11. Belfrage, P., Fredrikson, G., Olsson, H., and Stralfors, P. (1982) *Prog Clin Biol Res* **102**, 213-223
12. Greenberg, A. S., Egan, J. J., Wek, S. A., Garty, N. B., Blanchette-Mackie, E. J., and Londos, C. (1991) *J Biol Chem* **266**, 11341-11346
13. Fredrikson, G., Stralfors, P., Nilsson, N. O., and Belfrage, P. (1981) *J. Biol. Chem.* **356**,

6311-6320
14. Holm, C. (2003) *Biochem Soc Trans* **31**, 1120-1124
15. Yeaman, S. J. (2004) *Biochem J* **379**, 11-22
16. Egan, J., Greenberg, A., Chang, M.-K., Wek, S., Moos, J., MC, and Londos, C. (1992) *Proc. Natl. Acad. Sci., USA* **89**, 8537-8541
17. Londos, C., Sztalryd, C., Tansey, J. T., and Kimmel, A. R. (2005) *Biochimie* **87**, 45-49
18. Brasaemle, D., Levin, D., Adler-Wailes, D., and Londos, C. (2000) *Biochim Biophys Acta* **1483**, 251-262
19. Sztalryd, C., Xu, G., Dorward, H., Tansey, J., Contreras, J., Kimmel, A., and Londos, C. (2003) *J Cell Biol* **161**, 1093-1103
20. Tansey, J., Sztalryd, C., Gruia-Gray, j., Roush, D., Zeo, J., Gavrilova, O., Reitman, M., Deng, C.-X., Ki, C., Kimmel, A., and Londos, C. (2001) *Proc Natl Acad Sci, USA* **98**, 6494-6499
21. Martinez-Botas, J., Andreson, J., Tessler, D., Lapillojnne, A., Hung-Junn Chang, B., Quast, M., Gorenstein, D., Chen, K.-H., and Chan, L. (2000) *Nature Genetics* **26**, 474- 479
22. Souza, S., Muliro, K., Liscum, L., Lien, P., Yamamoto, Y., Schaffer, J., Dallal, G., Wang, X., Kraemer, F., Obin, M., and Greenberg, A. (2002) *J Biol Chem* **277**, 8267-8272
23. Zhang, H., Souza, S., Muliro, K., Kraemer, F., Obin, M., and Greenberg, A. S. (2003) *J Biol Chem* **278,** 51535-42
24. Brasaemle, D., Rubin, B., Harten, I., Gruia-Gray, J., Kimmel, A., and Londos, C. (2000) *J Biol Chem* **275**, 38486-38493
25. Moore, H. P., Silver, R. B., Mottillo, E. P., Bernlohr, D. A., and Granneman, J. G. (2005) *J Biol Chem* **280**, 43109-43120
26. Tansey, J., Huml, A., vogt, R., Davis, K., Jones, J., Fraser, K., Brasaemle, D., Kimmel, A., and Londos, C. (2003) *J Biol Chem* **278**, 8401-8406
27. Su, C. L., Sztalryd, C., Contreras, J. A., Holm, C., Kimmel, A. R., and Londos, C. (2003) *J Biol Chem* **278**, 43615-43619
28. Morimoto, C., Kameda, K., Tsujita, T., and Okuda, H. (2001) *J Lipid Res* **42**, 120-127
29. Brasaemle, D. L., Dolios, G., Shapiro, L., and Wang, R. (2004) *J Biol Chem* **279**, 46835-46842
30. Clifford, G., Londos, C., Kraemer, F., Vernon, R., and Yeaman, S. (2000) *J Biol Chem* **275**, 5011-5015
31. Clifford, G., Kraemer, F., Yeaman, S., and Vernon, R. (2001) *Metabolism* **50**, 1264-1269
32. Wang, J., Shen, W. J., Patel, S., Harada, K., and Kraemer, F. B. (2005) *Biochemistry* **44**, 1953-1959
33. Ohashi, M., Mizushima, N., Kabeya, Y., and Yoshimori, T. (2003) *J Biol Chem* **278**, 36819-36829
34. Ross, S. R., Graves, R. A., Greenstein, A., Platt, K. A., Shyu, H.-L., Mellovitz, B., and Spiegelman, B. M. (1990) *Proc. Natl. Acad. Sci.* **87**, 9590-9594
35. Brinster, R. L., Chen, H. Y., Trumbauer, M., Senear, A. W., Warren, R., and Palmiter, R. D. (1981) *Cell* **27**, 223-231
36. Rosen, E., Hsu, C.-H., Wang, X., Sakai, S., Freeman, M., Gonzalez, F., and Spiegelman, B. (2002) *Genes and Dev* **16**, 22-26
37. Martinez-deMena, R., Hernandez, A., and Obregon, M. J. (2002) *Am J Physiol Endocrinol Metab* **282**, E1119-1127
38. Klein, J., Fasshauer, M., Ito, M., Lowell, B. B., Benito, M., and Kahn, C. R. (1999) *J Biol Chem* **274**, 34795-34802
39. Souza, S. C., Yamamoto, M., Franciosa, M., Lien, P., and Greenberg, A. (1998) *Diabetes* **47**, 691-695
40. Gross, D. N., Farmer, S. R., and Pilch, P. F. (2004) *Mol Cell Biol* **24**, 7151-7162
41. Sokal, R. R., and Rohlf, F. J. (1969) *Biometry*, W. H. Freeman and Co., San Francisco, CA

42. Souza, S., Moitoso de Vargas, L., Yamamato, M., Line, P., Franciosa, M., Moss, L., and Greenberg, A. (1998) *J Biol Chem* **273**, 24665-24669
43. Marcinkiewicz, A., Gauthier, D., Garcia, A., and Brasaemle, D. L. (2006) *J Biol Chem* (Feb 17; [Epub ahead of print])

FOOTNOTES

# These authors contributed equally to the work in this paper.

[1] Abbreviations used are: AD, adiponectin; BAT, brown adipose tissue; DAG, diacylglyceride; DIC, differential interference contrast; FC, fat cake; FLAG, a peptide comprised of DYKDDDDK; GFP, green fluorescent protein; HSL, hormone sensitive lipase; IBMX, isobuthylmethylxanthine; IF, immunofluorescence; IP, immunoprecipitation; LD, lipid droplet; MEF, murine embryonic fibroblast; NE, norepinephrine; Nsdhl, NAD(P)H steroid dehydrogenase-like protein; Peri A, perilipin A; Peri AΔ1-6, perilipin A containing ser → ala mutations of all six PKA phosphorylation sites; Peri KO, perilipin knockout; PIA, phenyl isopropyl adenosine; PKA, protein kinase A; shRNA, small hairpin RNA; SP, cell supernatant remaining after removal of fat cake; TAG, triacylglyceride; WAT, white adipose tissue.

FIGURE LEGENDS

Fig. 1. Characterization of stable lines of MEF adipocytes derived from perilipin null (-/-) and wild type (+/+) mice. *(A)*, Expression profile of hallmark adipocyte proteins during the time-course of MEF differentiation. Total cell lysates were collected at the indicated day after induction of differentiation and equivalent protein loads were analyzed by Western blotting for perilipin, hormone sensitive lipase (HSL), and adiponectin (AD). Retrovirally expressed PPARγ is also shown. Protein lysates of Peri -/- and Peri +/+ adipocytes were subjected to all procedures (including exposure to film) at the same time and in the same apparati. *(B)*, Oil red O staining demonstrating neutral lipid (TAG) accumulation in Peri -/- MEF adipocytes. Peri -/- MEF adipocytes accumulate 20% less neutral lipid than MEF +/+ adipocytes. *(C),* Insulin-dependent glucose uptake in differentiated MEF adipocytes. Results are expressed as mean ± S.E. of three separate experiments performed in triplicate. 2DG, 2-[^{3}H]deoxyglucose.

Fig. 2. Mutation of PKA phosphorylation sites abrogates the ability of Peri A to promote PKA-stimulated lipolysis in Peri -/- MEF adipocytes. *(A)*, schematic diagram of Peri A and Peri AΔ1-6, a PKA phosphorylation mutant. Consensus PKA phosphorylation sites are indicated by arrows and numbered (1-6) according to convention. *(B),* Adenoviral (Ad) expression of Peri A and Peri AΔ1-6 in Peri -/- MEF adipocytes. *(C)*, Lipolysis assays. Peri -/- MEF cells were transduced with adenovirus expressing GFP (negative control), Peri A, or Peri AΔ1-6. After differentiation to adipocytes, cells were depleted of serum and treated for 2 h with/without forskolin. The medium was collected and glycerol content was determined. Results are expressed as mean ± S.E. of twelve separate experiments performed in duplicate or triplicate. *, $P < 0.01$ vs Ad GFP.

Fig. 3. HSL shRNA abrogates almost all PKA-dependent glycerol release in MEF adipocytes. Peri -/- MEFs were transduced with adenovirus (Ad) expressing either GFP (control), or Peri A in conjunction with either HSL shRNA or 'scrambled' shRNA. After differentiation to adipocytes, cells were treated for 2 h with/without forskolin. The medium was collected, and released glycerol was measured. *(A),* Western blot of endogenous HSL and adenovirally expressed Peri A in Peri -/-

MEF adipocytes. *(B),* Lipolysis assays demonstrating almost complete abrogation of perilipin-enhanced PKA-stimulated glycerol release in Peri -/- MEF adipocytes expressing HSL shRNA. Results are expressed as mean ± S.E. of six experiments performed in duplicate or triplicate. *, $P < 0.01$ vs Ad GFP.

Fig. 4. Mutation of PKA phosphorylation sites in Peri A does not abrogate HSL translocation to LDs. Peri -/- MEFs were transduced with adenovirus and differentiated to adipocytes (as in Fig. 2). Following serum depletion, MEF adipocytes were treated for 15 min with/without forskolin plus IBMX followed by either *(A)* cell fractionation to obtain fat cake (FC) and supernatant (SP) fractions followed by Western blotting for HSL and perilipin, or *(B)* immunostaining with anti-HSL antibody (green) and analysis by immunofluorescence (columns 1 and 3) and differential interference contrast microscopy (columns 2 and 4). Note that in the presence of either Peri A or Peri AΔ1-6, PKA activation by forskolin leads to a relative increase in HSL in the FC fraction (Western blot) or associated with LDs (bright, LD-localized green in confocal images), coincident with reduced levels of HSL associated with the SP fraction (Western blot) and non-LD cell compartments (confocal images). Shown are representative data from 2-5 cell fractionation and seven confocal experiments.

Fig. 5. **PKA-stimulated glycerol release is blunted in differentiated brown adipocytes from Peri AKOΔ1-6 mice**. *(A),* Western blotting for protein markers of brown adipocyte differentiation in wild type and Peri AKOΔ1-6 mice. Brown pre-adipocytes from wild type and Peri AKOΔ1-6 mice were differentiated to adipocytes. Cell extracts (20 μg) were immunoblotted with antibodies recognizing Peri A, the FLAG epitope ligated to Peri AΔ1-6, phosphorylated serine and threonine residues of PKA substrates (~P-PKA substrate), HSL or UCP1. One of two replicate blots. *(B)*, Lipolysis assay. Cells were treated with PIA (basal) or with norepinephrine (NE, 10 μM) for 40 min after which media were collected and assayed for glycerol. Results represent the mean ± S.E. of sextuplicate measurements. ***, $P < 0.001$ vs basal; *, $P = 0.02$ vs basal.

Fig. 6. Differentiated brown adipocytes from Peri AKOΔ1-6 mice exhibit catecholamine-induced HSL translocation. Differential interference contrast (DIC) and immunofluorescence (IF) images of differentiated brown adipocytes from wild type and Peri AKOΔ1-6 mice treated with PIA (basal) or with norepinephrine (NE, 10 μM) for 15 min, followed by immunostaining for perilipin (PERI, red) and HSL (green). Co-localization of HSL and perilipin is indicated by the yellow/orange color in the PERI / HSL overlay. Data shown are representative of two individual experiments. Scale bar represents 8.3 μm.

Fig. 7. Crosslinking of HSL and perilipin is enhanced following PKA activation and is blunted in Peri -/- MEF adipocytes expressing Peri AΔ1-6. Peri -/- MEF adipocytes adenovirally-expressing GFP, FLAG tagged Peri A or FLAG tagged Peri AΔ1-6 were treated for 15 min with/without the PKA activator forskolin. Lipid droplets were released from cells by homogenization and LD-associated proteins were solubilized with detergent (see Experimental Methods). Detergent lysates were treated with crosslinker (DTSSP) followed by perilipin immunoprecipitation (IP) with anti-FLAG agarose beads. Following the breaking of protein crosslinks by 2-mercaptoethanol, *(A)* immunoprecipitates were analyzed by Western blotting for the presence of perilipin and co-immunoprecipitated HSL. One of four similar experiments is shown. *(B)* Western blot of perilipin immunoprecipitates (20% input, lanes 1-6) and the pre-IP lysate from MEF adipocytes expressing Peri A (5% input, lane 7) for the LD-associated protein NAD(P)H steroid dehydrogenase-like protein (Nsdhl). One of two similar experiments is shown.

TABLE I

Effect of Peri A and Peri A phosphorylation on HSL distribution in MEF adipocytes

HSL Western blots (as in Fig. 4A) were quantified by scanning laser densitometry. Superscripts denote the following comparisons: 1, vs. GFP, $p < 0.001$; 2, vs. basal, $p < 0.05$; and 3, vs. basal, $p < 0.01$.

		Basal		+ Forskolin	
Cell fraction		FC	SP	FC	SP
Ad GFP	(n=2)	8.3 ± 6.2	91.7 ± 6.2	4.7 ± 0.5	95.3 ± 0.5
Ad PeriA	(n=5)	49.8 ± 4.0[1]	50.2 ± 4.0	62.6 ± 2.8[2]	37.4 ± 2.8
Ad Peri A 1-6	(n=4)	46.0 ± 1.5[1]	54.0 ± 1.5	66.8 ± 8.2[3]	33.2 ± 8.2

Fig. 1

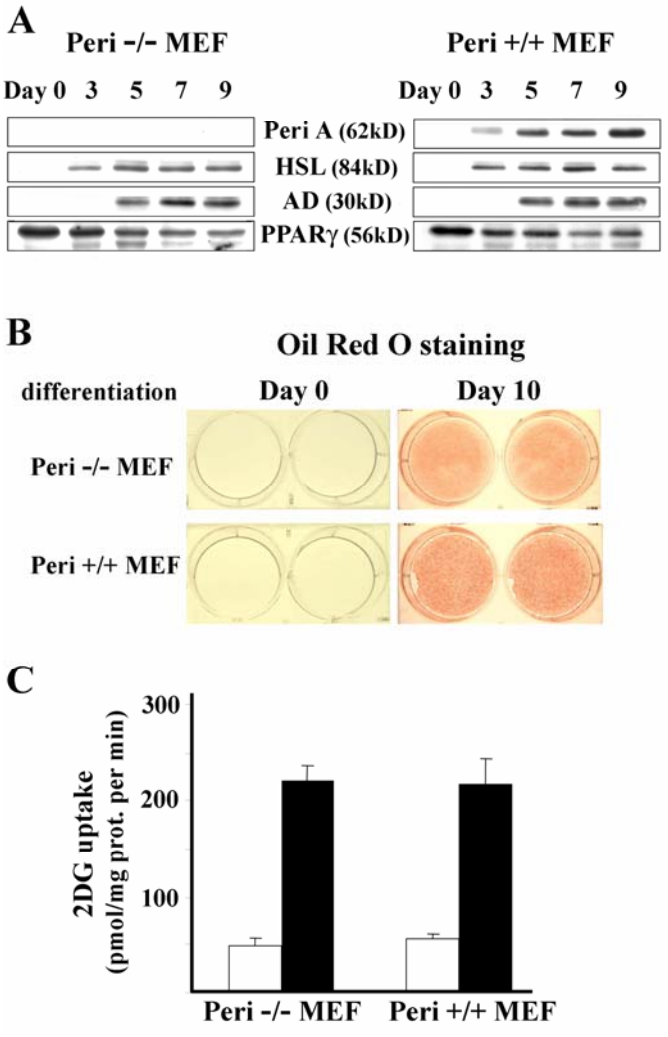
A
Peri -/- MEF
Peri +/+ MEF
Day 0 3 5 7 9
Day 0 3 5 7 9
Peri A (62kD)
HSL (84kD)
AD (30kD)
PPARγ (56kD)
B
Oil Red O staining
differentiation
Day 0
Day 10
Peri -/- MEF
Peri +/+ MEF
C
2DG uptake
(pmol/mg prot. per min)
300
200
100
Peri -/- MEF
Peri +/+ MEF

Fig. 2

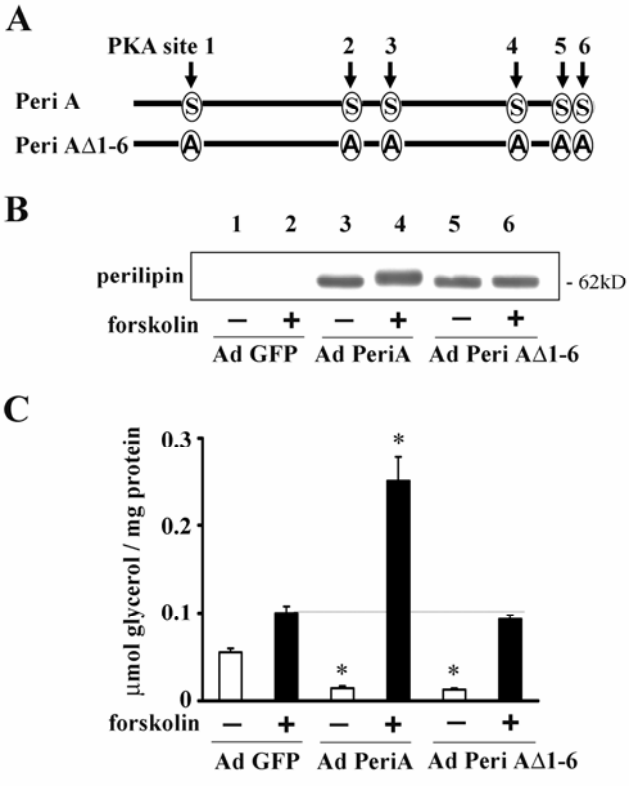
A
PKA site 1
2
3
4
5
6
Peri A
Peri AΔ1-6
S
A
B
1
2
3
4
5
6
perilipin
- 62kD
forskolin
– + – + – +
Ad GFP
Ad PeriA
Ad Peri AΔ1-6
C
μmol glycerol / mg protein
0.3
0.2
0.1
0
*
forskolin
– + – + – +
Ad GFP
Ad PeriA
Ad Peri AΔ1-6

Fig. 3

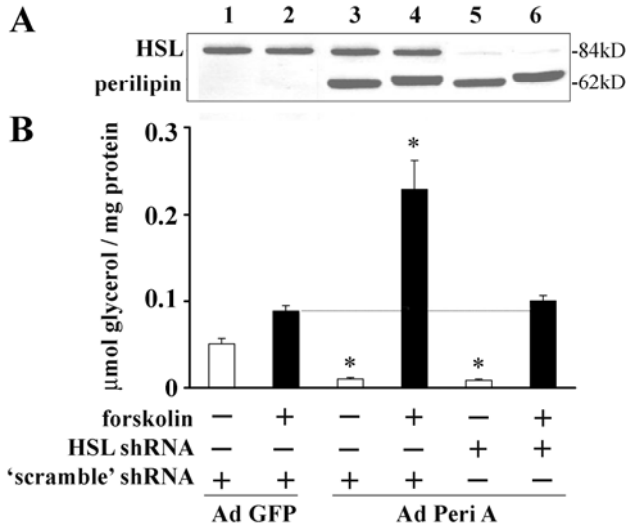
A
1
2
3
4
5
6
HSL
perilipin
-84kD
-62kD
B
µmol glycerol / mg protein
0.3
0.2
0.1
0
*
*
*
forskolin − + − + − +
HSL shRNA − − − − + +
'scramble' shRNA + + + + − −
Ad GFP
Ad Peri A

Fig. 4

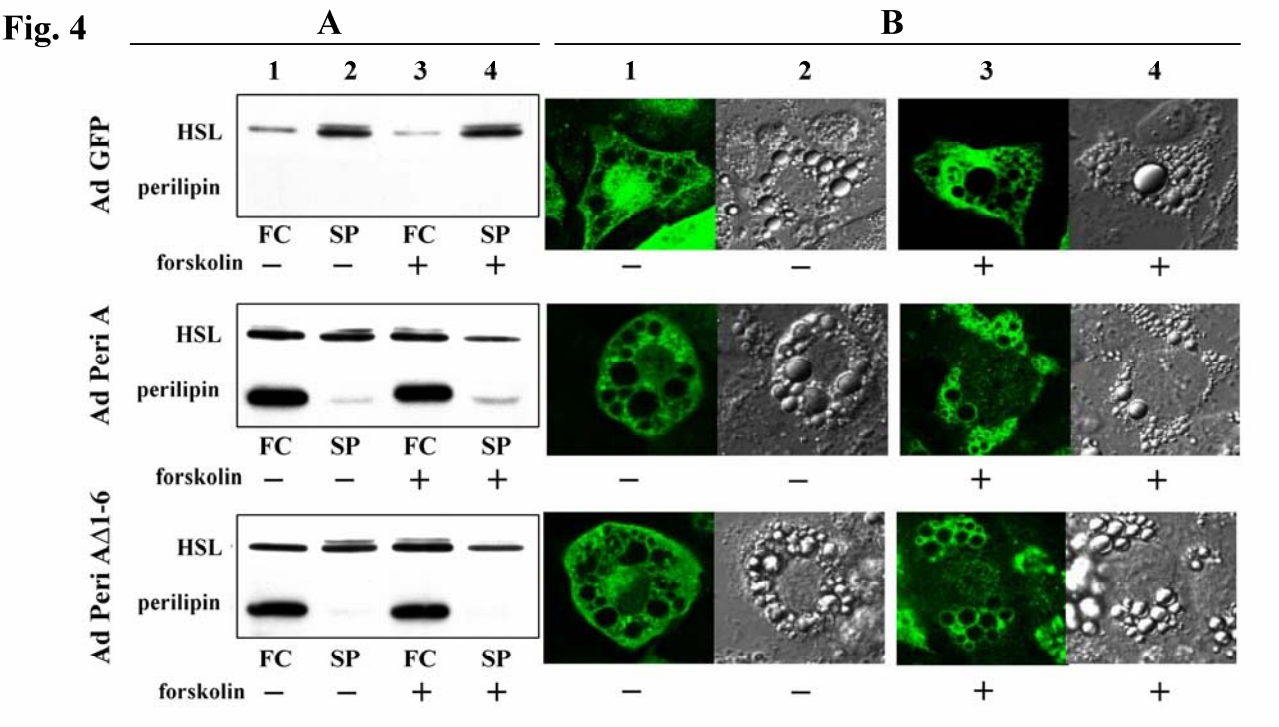
A
B
1
2
3
4
Ad GFP
Ad Peri A
Ad Peri AΔ1-6
HSL
perilipin
FC
SP
forskolin
–
+

Fig. 5

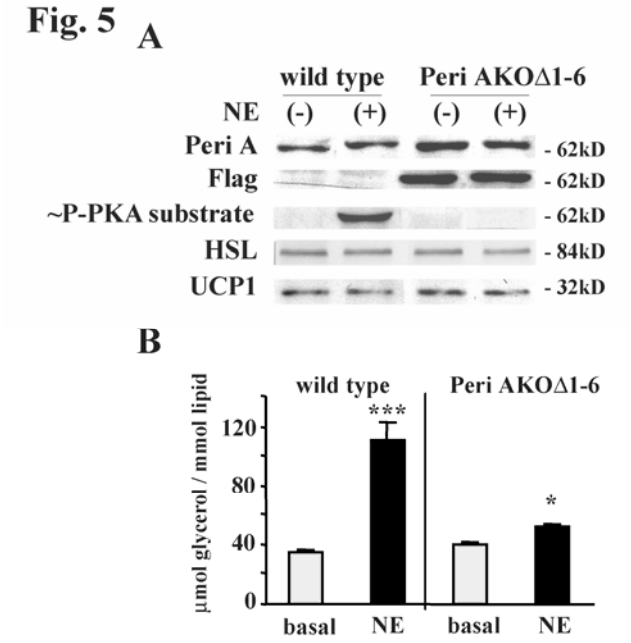
A
wild type
Peri AKOΔ1-6
NE
(-)
(+)
(-)
(+)
Peri A
- 62kD
Flag
- 62kD
~P-PKA substrate
- 62kD
HSL
- 84kD
UCP1
- 32kD
B
wild type
Peri AKOΔ1-6
µmol glycerol / mmol lipid
120
80
40
0
***
*
basal
NE
basal
NE

Fig. 6

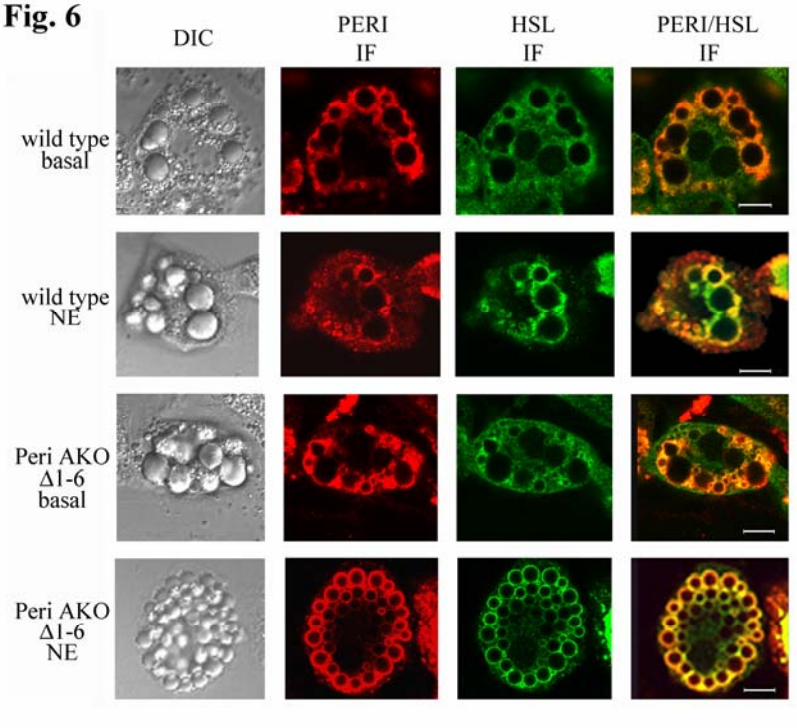
DIC
PERI IF
HSL IF
PERI/HSL IF
wild type basal
wild type NE
Peri AKO Δ1-6 basal
Peri AKO Δ1-6 NE

Fig. 7

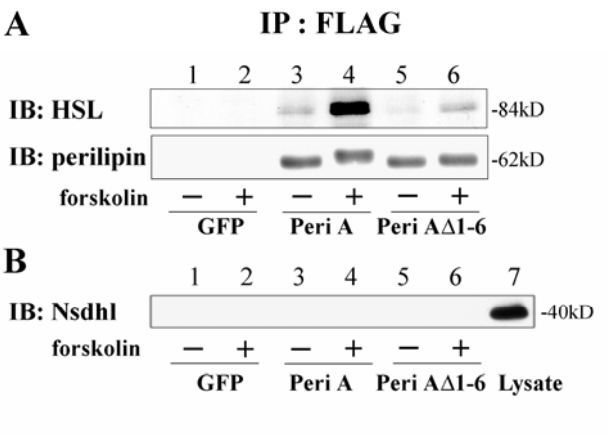
A
IP : FLAG
1 2 3 4 5 6
IB: HSL
-84kD
IB: perilipin
-62kD
forskolin − + − + − +
GFP
Peri A
Peri AΔ1-6
B
1 2 3 4 5 6 7
IB: Nsdhl
-40kD
forskolin − + − + − +
GFP
Peri A
Peri AΔ1-6
Lysate